DIAGNOSE EYES DISEASES USING VARIOUS FEATURES EXTRACTION APPROACHES AND MACHINE LEARNING ALGORITHMS

Zahraa Najm Abed[1]
[1] *Informatics Institute for Postgraduate Studies, Iraqi Commission for Computers and Informatics (ICCI)*
ms202120673@iips.icci.edu.iq

Abbas M Al-Bakry [2]
University of Information Technology and Communication (UOITC)
abbasm.albakry@uoitc.edu.iq

Abstract
Ophthalmic diseases like glaucoma, diabetic retinopathy, and cataracts are the main cause of visual impairment worldwide . With the use of the fundus images, it could be difficult for a clinician to detect eye diseases early enough. By other hand, the diagnoses of eye disease are prone to errors, challenging and labor-intensive. Thus, for the purpose of identifying various eye problems with the use of the fundus images, a system of automated ocular disease detection with computer-assisted tools is needed. Due to machine learning (ML) algorithms' advanced skills for image classification, this kind of system is feasible. An essential area of artificial intelligence(AI) is machine learning. Ophthalmologists will soon be able to deliver accurate diagnoses and support individualized healthcare thanks to the general capacity of machine learning to automatically identify, find, and grade pathological aspects in ocular disorders. This work presents a ML-based method for targeted ocular detection. The Ocular Disease Intelligent Recognition (ODIR) dataset, which includes 5,000 images of 8 different fundus types, was classified using machine learning methods. Various ocular diseases are represented by these classes. In this study, the dataset was divided into 70% training data and 30% test data, and preprocessing operations were performed on all images starting from color image conversion to grayscale, histogram equalization, BLUR, and resizing operation. The feature extraction represents the next phase in this study, two algorithms are applied to perform the extraction of features which includes: SIFT(Scale-invariant feature transform) and GLCM(Gray Level Co-occurrence Matrix), ODIR dataset is then subjected to the classification techniques Naïve Bayes, Decision Tree, Random Forest, and K-nearest Neighbor. This study achieved the highest accuracy for binary classification (abnormal and normal) which is 75% (NB algorithm), 62% (RF algorithm), 53% (KNN algorithm), 51% (DT algorithm) and achieved the highest accuracy for multiclass classification (types of eye diseases) which is 88% (RF algorithm), 61% (KNN algorithm) 42% (NB algorithm), and 39% (DT algorithm).

Index Terms - Machine Learning, Random Forest, Naïve Bayes, K-nearest Neighbor, ODIR.

I. INTRODUCTION

Diagnosing ocular pathology utilizing the fundus images represents a considerable difficulty in the healthcare field[1] . Ocular diseases can be defined as any disorder or condition interfering with the capacity of the eyes to correctly operate or has detrimental impacts on the visual acuity of the eyes, nearly all people experience visual issues at some point in their lives. Others require the care of an expert, whereas some are minors which don't appear on claims or can simply be treated at home[2].

worldwide, fundus disorders represent the key reason why people become blind. The most prevalent ocular diseases include cataract, age-related macular degeneration (AMD), glaucoma, diabetic retinopathy (DR). By 2030, there would be more than 400 million people with DR, say the studies that are related[3].

Those ocular conditions are now a significant global healthcare issue. Most importantly, the ophthalmic condition is fatal and can leave the patients blind permanently. In the clinical settings, the early detection of those illnesses can prevent the vision impairments. Therefore, automated computer-aided diagnostic approaches are crucial for the identification of the eye problems[3].

One of the most important steps in minimizing an ophthalmologist's workload is the automatic diagnosis of illnesses. Medical institutions are constantly in need of computerized assistance to help them diagnose specific illnesses more accurately. This assistance could be in the form of large-scale data collection, complex input analysis, data organization and classification, relationship discovery, and a host of other tasks that might benefit greatly from computerization. Diseases could be detected using ML and computer vision technology without the need for human interaction. Even while numerous studies have produced encouraging findings, very few of them were able to fully diagnose multiple eye diseases. To accurately diagnose diverse eye conditions, more investigation into the many features of fundus imaging is required. This study suggests a ML-based system for classifying different eye illnesses.

The remainder of the study is structured as follows: first, a quick explanation of the database employed. The procedures for preprocessing and feature extraction are then described. The machine learning techniques utilized for predicting eye diseases are explained in section three. The study is completed after the results are discussed in section four.

II. II. RELATED WORK

Krishna Prasad; M Neema; P S Sajith; P N Priya; Lakshmi Madhu 2019[4]. The authors develop a model Multiple eye disease detection using DNN (The suggested DNN model is helpful in early detection of glaucoma and diabetic retinopathy. It may prompt patients to seek out an ophthalmologist for

screening purposes. The created model was simpler and produced an accuracy of 80%).

N. Gour and P. Khanna,2021 [5].The authors apply multi-class multi-label ophthalmological disease detection utilizing the transfer learning based CNN. The suggested approach implements 4 state-of-the-art pretrained CNN models for their fine-tuning on the ODIR data-base. Parametric assessments of the validation, training, and testing phase showed that VGG-16 network works better compared with the ResNet , Inception V3, and MobileNet CNN architectures. F-1 and AUC score achieved with VGG-16 for 2 input methods with the SGD optimizer were 85.57 and 84.93, respectively. The concatenated input approach with VGG-16 architecture, known as the Model2, which has shown as wekk better AUC and F-1 score, i.e., 68.88 and 85.57 with the VGG-16 utilizing the SGD optimizer compared with other architecture.

Nouf Badah, Amal Algefes, Ashwaq AlArjani and Raouia Mokni 2022 [6]. The authors performed automatic detection of eye diseases utilizing deep learning and ML models. The approaches of classification based upon 6 ML approaches is K-Nearest Neighbors (KNNs), Support Vector Machine (SVM), Naïve Bayes (NB), Decision Tree (DT), Multi-layer perceptron (MLP), and Random Forest (RF). and secondly a Deep Learning (DL) model such as Convolutional Neural Network (CNN) based on Resnet152 model. The evaluation of the suggested approach has been performed on (ODIR) dataset. The collected findings demonstrated that, compared with the other ML classifiers, the MLP and RF classifiers had the best accuracy of 77%. For the identical task and data-set, the DL model (CNN model: Resnet-152) offers an even higher level of accuracy of 84%for the same task and data-set.

TABLE I
THE SUMMARY OF PREVIOUS WORKS ABOUT EYES DISEASES

Authors	Year	Proposed method	Accuracy
Krishna Prasad; M Neema; P S Sajith; P N Priya; Lakshmi Madhu [4]	2019	DNN model	80%
N. Gour and P. Khanna **[5]**	2021	CNN models (VGG- 16, ResNet, Inception V3, and MobileNet)	85.57% (VGG-16)
Nouf Badah, Amal Algefes, Ashwaq AlArjani and Raouia Mokni [6]	2022	Deep learning (CNN model: Resnet-152) and ML models (KNNs,SVM,NB,DT,MLP,RF)	84% (CNN)

III. PROPOSED SYSTEM

Figure 1 below shows a model diagram of the suggested process.

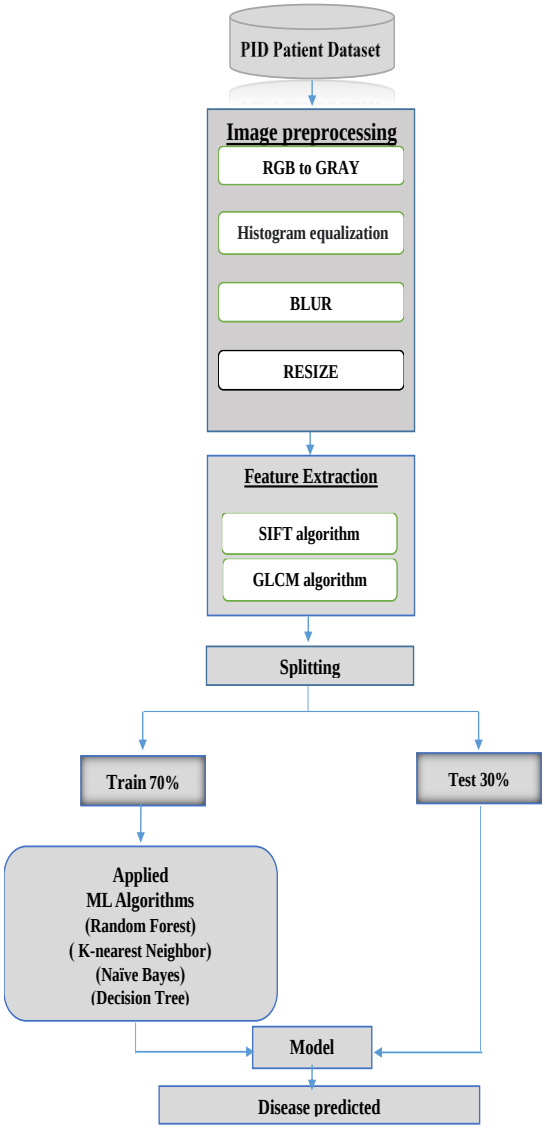

Fig. 1. Proposed Model Diagram

IV. DATASET USED:

This study's main objective is to utilize the medical database Ocular Disease Intelligent Recognition (ODIR) to predict which patients would have eye illnesses.

TABLE II
BRIEF DATASET DESCRIPTION

Database	No. of Attributes	No. of Instances
PID	19	5,000

This database is from Kaggle. A structured ophthalmic data-base that consists of 5000 persons containing age, color fundus images of the left and right eyes, and diagnostic key-words from doctors is called ODIR. This data-set is intended to reflect a "real-life" set of patient data which Shang gong Medical Technology Co., Ltd. gathered from a variety of the medical facilities and hospitals in China. Those institutions utilize various cameras that are available on the market, which

includes Zeiss, Canon, and Kowa, to acquire fundus images, producing images with different image resolutions. With quality control management, trained human readers assigned labels to the annotations. Patients have been divided to 8 labels, including:

- Normal (N),
- Glaucoma (G),
- Diabetes (D),
- Pathological Myopia (M),
- Age related Macular Degeneration (A),
- Hypertension (H),
- Cataract (C),
- Other diseases/abnormalities (O).

V. PREPROCESSING PROCEDURES:

Image preprocessing is a substantial research topic, and the attaining of the images has been increased in a multi number of applications. Digital image preprocessing refers to a set of operations that must be performed on the inputted image to the Diagnose system to improve it before performing any other techniques and methods on the image. The need for the preprocessing is significant, due to the need of reducing any superfluous data for the benefit of being willing in the afterword phases of the Diagnose system [7].

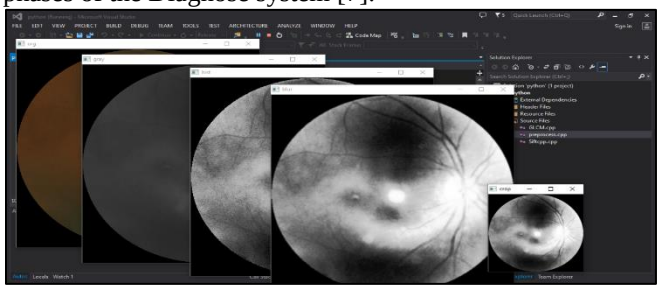

Figure2,3 Shows Image preprocessing

A. Convert the image to greyscale color space

The inputted image undergoes a color change at the introduced time, going from an RGB colour space imitation to a different one referred to as gray-scale colour space. This conversion takes place due to the fact that an image in RGB (Red, Green, & Blue) colour space needs 3 channels to be saved then represented in a computer, while an image in grey-scale color space requires 1 channel only. The objective of such conversion is using less data for representing an image. The speed of the processing is accelerated through the turning of the colored images to gray-scale. This gray-scale image, naturally, has an intensity which is saved as eight-bit integer value, which provides 256 different options for grey spectra, which range from the ones that are white to those that are black. Each one of the pixels of inputted eye image, which has 24bits, is converted to gray-scale color pixels which have just eight bits, at this stage of image preprocessing.

The next equation has been utilized for the conversion of an image from RGB to grey modes [8]:

GRAY = 0.30 R + 0.59G + 0.11 B..... (1)

Figure4 Shows convert image to gray level

B. Histogram equalization

The histogram equalization (HE) approach has proven to be a very accurate way to combine brightness and color data obtained from important local characteristics in color images. Additionally, it does a fantastic job of lowering contrast, noise, and blurriness [9]. The HE (histogram equalization) method is utilized to increase the contrast in an image. Its fundamental idea is to map gray levels with the use of the input gray level probability distribution as a guide. Through flattening and extending the image histogram's dynamic range, it enhances overall contrast [10]. Images with a simple background and foreground intensity and either a bright or dark background and foreground tend to function well with this technique [11]. The next equation illustrates how to compute HE (histogram equalization) using the histogram cumulative distribution function[12].

$$\text{Cdf (X)} = \sum_{i=1}^{x} \text{h}(i) \text{..... (2)}$$

Where X represent the gray value and h illustrate the image's histogram.

$$\text{T[pixel]} = \text{round}\left(\left(\frac{cdf(x) - cdf(x)_{min}}{E*F - cdf(x)_{min}}\right) * (\text{L} - 1)\right) \text{..... (3)}$$

$cdf(x)_{min}$: is the minimum value of the cumulative distribution function.

E * F: Columns and rows number of images

L: Gray levels used =256.

Figure5 shows the result of histogram equalization of the gray image

C. Blurring

By convolutioning the image with a low pass filter kernel, blurring is achieved. Smoothing images for the purpose of eliminating texture or noise in small details is advantageous in noise elimination. Applying image processing methods that focus on the image's finer details is typically advantageous [13]. There are various techniques to carry out this operation. The typical filter types utilized in these techniques include:

- Mean filter
- Median filter
- Gaussian filter

In this work using the Gaussian filter(5×5).

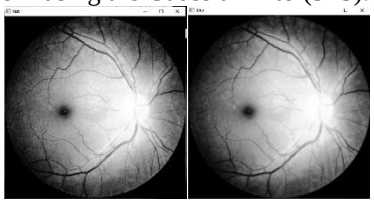

Figure6 shows the blurring result

D. Resize image

Figure (5) illustrate the eye image after resizing process. In this work using the Bicubic Interpolation[14], All images were reshaped with (200*200) distances.

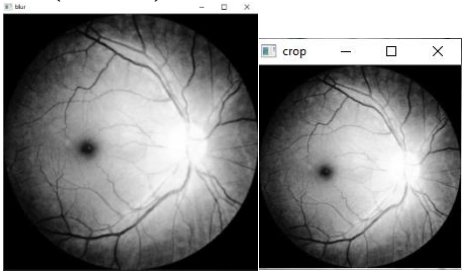

Figure7 shows the resizing result

VI. FEATURE EXTRACTION

Feature extraction can be considered as a certain type of dimensionality reduction utilized in the process of image processing and pattern recognition. Finding the most relevant information in the original data and representing it in lower dimensional space represent the main goals of the feature extraction[15].

Input data will be transformed to reduced representation set of the features (which is known as a features vector as well) in the case where input data to the algorithm is too vast to be processed and it's considered as redundant (much data, but not that much information). The transformation of input data to the feature set has been referred to as the feature extraction. In the case where extracted features are chosen correctly, it's anticipated that feature set will extract necessary data from input to perform intended task with the use of this reduced representation rather than the full-size input[16].

❖ SIFT (Scale-invariant feature transform) Features Extraction

In 1999, Lowe developed the SIFT technique for addressing the issue of invariance to the rotation and scaling in the process of feature extraction [17],[18] . Translation, scaling, rotation, and variation in the conditions of illumination have little effect on SIFT descriptors. Furthermore, they exhibit some affine distortion invariance. Image classification is just one of the many computer vision applications that can make use of SIFT features. After extracting the features from the image to be examined, a match is made with features that are stored in a data-base of recognized objects. Additionally, localization, 3D mapping, recognition, scene modeling, and tracking may all be done using SIFT characteristics [19]–[22].

There are 4 SIFT features detection steps:

1-Scale-space extrema detection: In first stage, a DoG function is used for scanning all of the image locations and scales in order to look for potential interest points regardless of the scale and orientation.

2. Keypoint localization: With the use of two distinct types of thresholds, low contrast areas and edges are removed from the locations from the first stage.

3. Orientation assignment: According to the local image gradient directions, each key point is given at least one orientation. Since all ensuing operations are carried out on image data that was adjusted to the stated scale, orientation, and location for each feature, transformations are invariant.

4. Keypoint descriptor: For the area surrounding each keypoint, a local feature description has been calculated. Each one of the feature descriptors is a vector of 128 dimensions that specifically identifies the region around the keypoint. To provide orientation invariance, the descriptor has been based upon a local image gradient that was rotated based on keypoint orientation.

Some of these descriptors must be employed because real world images often have numerous SIFT-generated attributes.

❖ GLCM (Gray Level Co-occurrence Matrix) Features Extraction

It is generally known that second-order statistical texture features can be extracted from images by applying statistical intensity combination distributions at different points around each other [23], [24]. Statistics come in three different orders, depending on the number of the intensity points that are present in an image. Though theoretically feasible, implementation of higher orders statistics is impossible due to computational cost. Information regarding structural organization of surfaces and their interactions to their surroundings is contained in texture features [25]. We acquire a total of 22 texture-based features, like inverse difference moment (IDM), correlation, energy, entropy, variance of sum, homogeneity, contrast, dissimilarity, autocorrelation, maximal probability, and IDM normalized, amongst a lot others. Some of them are formulated as follows:

Energy:

'Uniformity' or 'angular second moment' are other words for energy. It provides the GLCM matrix's square element summation. Through homogenous regions to the non homogeneous regions is the way it works. It is high in the case where the repeated image pixels occur frequently.

$$Energy = \sum_{i,j=0}^{N-1} \left(P_{ij}\right)^2 \ldots. (4)$$

Entropy:

It determines image's randomness. A homogeneous image will therefore have lower values of entropy.

$$Entropy = \sum_{i,j=0}^{N-1} -ln(p_{ij})P_{ij} \ldots. (5)$$

Contrast:

It quantifies degree of the contrast between the pixel and its surrounding pixels throughout the whole image.

$$Contrast = \sum_{i,j=0}^{N-1} P_{ij}(i-j)^2 \ldots. (6)$$

Correlations:

It represents a measurement of image's linear gray tone dependence. It describes correlation between the pixel and its neighbor.

$$Correlation = \sum_{i,j=0}^{N-1} P_{ij} \frac{(i-\mu)(j-\mu)}{\sigma^2} \ldots. (7)$$

Homogeneity:

It specifies about how similar pixels are. The homogenous image's GLCM matrix indicates that its value is 1. If the image texture only needs minor adjustments, it is extremely low.

$$Homogeneity = \sum_{i,j=0}^{N-1} \frac{P_i j}{1+(i-j)^2} \ldots. (8)$$

Where

Pij= (i,j) the normalized GLCM matrix element.

μ= average GLCM matrix that had been computed with the use of the equation

$$\mu = \sum_{i,j=0}^{N-1} iP_{ij} \ldots. (9)$$

σ= represents intensity variance of all of pixels that have been calculated using

$$\sigma^2 = \sum_{i,j=0}^{N-1} P_{ij}(i-\mu)^2 \ldots. (10)$$

N= No. of grey levels in an image.

VII. BRIEF DESCRIPTION OF ALGORITHMS USED:

1) Naïve Bayes (NB):

The base of the NB classification method is the notion that each feature exists independently of the others. According to this, the status of one characteristic within a class is unaffected by the status of another characteristic. Due to the fact that it has been based upon the conditional probability, it has been considered as powerful method for classification [26]. The Naive Bayesian is affected by this: the probabilities P (C n) of each of these classes are assessed from training data-set and show the likelihood of the classification of Vj attribute to each of the C n classes as a result of the Cn classes. This likelihood is demonstrated by the classification employed in the following equation for the Vj attribute value [27]:

$$\frac{P(v_1 \wedge v_2 \ldots\ldots v_j \mid c_n)P(c_n)}{P(v_1 \wedge v_2 \ldots\ldots v_j)} \quad \ldots\ldots\ldots\ldots\ldots\ldots (11)$$

2) K-nearest Neighbor (KNN):

One of the most popular instance-based learning approaches for process of pattern recognition, it's a supervised learning algorithm. K-NN is a lazy learner who works well when all of the data is the same size because it lacks a training phase. As a result of its simplicity, KNN concept became one of the popular tools for the classification in a wide variety of the applications [28]. Manhattan and Euclidean distances represent the two best distance measures that are utilized by KNN algorithm:

$$D(X_q, X_i) = \sqrt{\sum nr} = 1(ar(X_q) - ar(X_i)^2 \ldots\ldots. (12)$$

$$D(X_q, X_i) = \sqrt{\sum nr} = 1(ar(X_q) - ar(X_i)^| \ldots\ldots (13)$$

In which X stands for the input and is represented by n-dimensional feature vector (a1, a2, a3,... an), Xq for query vector, i for training data's index vector, and ar for the vector X function's number value.

3) Decision Tree (DT) Algorithm

DTs are among the most important techniques used in a number of fields, such as image processing and pattern recognition. DT represents a sequential model which successfully and cogently connects a number of basic tests wherein each test compares numerical feature with threshold value. Furthermore, compared to conceptual principles, the creation of numerical weight values for the neural network's connections between nodes is far more challenging. DT is mostly used for grouping objectives. Additionally, DT is a common classification model in the process of data mining. The nodes and branches make form the structure of each tree. Each of the subsets designates a possible value for the node, and each node identifies the characteristics of a category into which it should be classified. Due to its accuracy and ease of analysis across a variety of data formats, DTs also have various applications. Entropy is a measurement of a dataset's randomness or impurity. Entropy values range from 0 to 1. According to equation (2.2), when it equals 0, it is better, and when it equals 1, it is worse [29]:

$$Entropy(p) = \sum_{i=1}^{c} p_i \log 2^{pi} \ldots\ldots (14)$$

In which Pi=(p1, p2,..., pn) Probability of distinct class and P denotes attribute (class). It is possible to define information gain as one of the metrics that may be used to assess the level of class mixing in each sample, and consequently at any stage of the tree's growth. As stated in equation (2.3), a function must still be created to determine which test will label the present node [30]:

$$\text{Gain(p, T)} = \text{Entropie(p)} - \sum_{i=1}^{n} (P_j \times \text{Entropie}(P_j)) \ldots\ldots (15)$$

Where the values (p_j) stand in for the entire set of possible values for the characteristic T. Such metrics could be used to rank characteristics and create the DT, where each node finds the attribute with the maximum information gain among the attributes that haven't yet been stated along the path from the root.

4) Random Forest (RF) Algorithm

RF is a member of the family of algorithms referred to as "bagging" (short for "bootstrap aggregating"). They give the user the option of creating the best decision trees by combining a number of iterative trees that were constructed from randomly selected training step samples. Increased prediction on the noisy datasets is possible by the aggregation and construction of small trees from the small subset. This algorithm's general idea is to build a few computationally inexpensive features for small decision trees. If we might simultaneously construct a large number of little DTs, we could after that combine or vote to combine the trees into a single, powerful learner [31].

VIII. PERFORMANCE MEASURES:

Various metrics were used for the evaluation of the performance of the system.

A. Precision: is the amount of true positive elements that are separated by the number of true positive elements and number of false positive cases, Which are examples of the model that exactly label it as positive, which are actually negative or which are classified in our example as terrorists [32].

$$\text{Precision}=\frac{TP}{TP+FP} \dots\dots (16)$$

Where TP: True Positive and FP: False Positive cases

B. Recall: The ability to locate all of the relevant examples in a dataset is the ratio of the data points that were relevant in this model states [33].

$$Recall = \frac{TP}{TP+FN} \dots\dots (17)$$

C. F-measure: The test has been used in order to determine grade, and the precision measure called the F (or F-measure) is employed. The number of successful outcomes divided by the total number of the positive outcomes has been referred to as accuracy of p, and the number of the positive cases divided by entire number of the positive outcomes is known as retrieval r. With F-1 being the best at one and worst at 0, FF (mean F1) is a harmonic intermediate accuracy and recall value. The general formula demands a true positive β, therefore for a user who hangs β importance times, the accuracy of the recovery efficacy is measured by the F-score [34].

$$F_1 = \frac{1}{\frac{1}{recall}+\frac{1}{precision}} = 2*\frac{precision*recall}{precision+recall} \dots\dots\dots (18)$$

RESULTS

In this section, results are presented, which have been obtained after dividing the data-set into testing and training, 30% for test and 70% for train, After applying preprocessing and feature extraction operations(in Microsoft Visual Studio Ultimate 2013), then applying machine learning algorithms(in Python IDLE (V. 3.6.5)) for the purpose of obtaining overall prediction results.

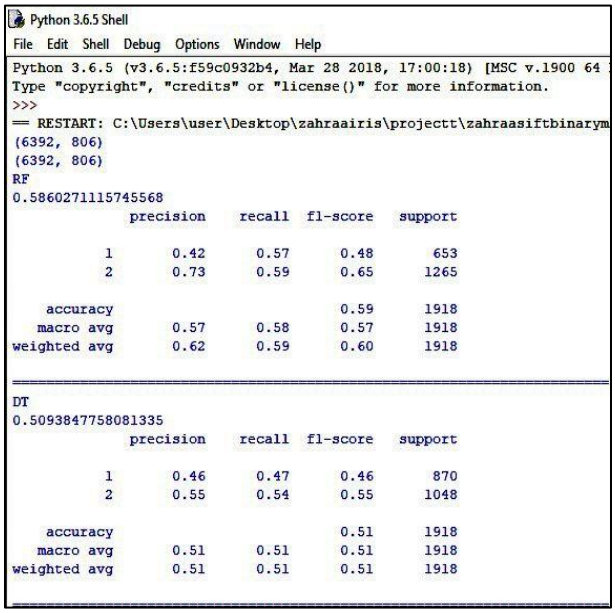

```
Python 3.6.5 Shell
File  Edit  Shell  Debug  Options  Window  Help
Python 3.6.5 (v3.6.5:f59c0932b4, Mar 28 2018, 17:00:18) [MSC v.1900 64
Type "copyright", "credits" or "license()" for more information.
>>>
== RESTART: C:\Users\user\Desktop\zahraairis\projectt\zahraasiftbinarym
(6392, 806)
(6392, 806)
RF
0.5860271115745568
              precision    recall  f1-score   support

           1       0.42      0.57      0.48       653
           2       0.73      0.59      0.65      1265

    accuracy                           0.59      1918
   macro avg       0.57      0.58      0.57      1918
weighted avg       0.62      0.59      0.60      1918

DT
0.5093847758081335
              precision    recall  f1-score   support

           1       0.46      0.47      0.46       870
           2       0.55      0.54      0.55      1048

    accuracy                           0.51      1918
   macro avg       0.51      0.51      0.51      1918
weighted avg       0.51      0.51      0.51      1918
```

Fig. 8

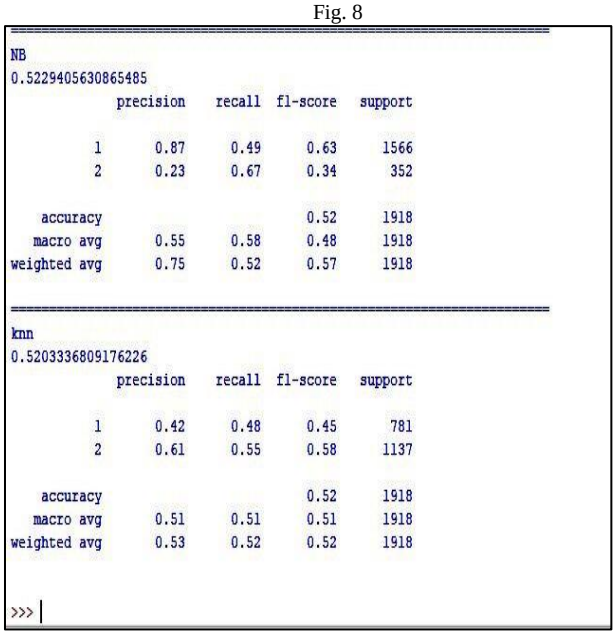

```
NB
0.5229405630865485
              precision    recall  f1-score   support

           1       0.87      0.49      0.63      1566
           2       0.23      0.67      0.34       352

    accuracy                           0.52      1918
   macro avg       0.55      0.58      0.48      1918
weighted avg       0.75      0.52      0.57      1918

knn
0.5203336809176226
              precision    recall  f1-score   support

           1       0.42      0.48      0.45       781
           2       0.61      0.55      0.58      1137

    accuracy                           0.52      1918
   macro avg       0.51      0.51      0.51      1918
weighted avg       0.53      0.52      0.52      1918

>>>
```

Fig. 9

Fig8,9 shows the results of binary classification

TABLE III
CLASSIFIER'S PERFORMANCE ON THE CLASSIFICATION ALGORITHMS

classification algorithms (binary classification)	Precision	Recall	F1-measure
Naïve Bayes (NB)	75%	52%	57%
Random Forest (RF)	62%	59%	60%
K-nearest Neighbor (KNN)	53%	52%	52%
Decision Trees (DT)	51%	51%	51%

As illustrated in the previous table the results show precision values in the (ODIR) dataset that appears the NB algorithm scored the highest precision in ML(machine learning)

algorithms that is 75% compared to the RF algorithm that achieves 62%, the KNN algorithm that achieves 53% and the DT algorithm that achieves 51% in case of binary classification.

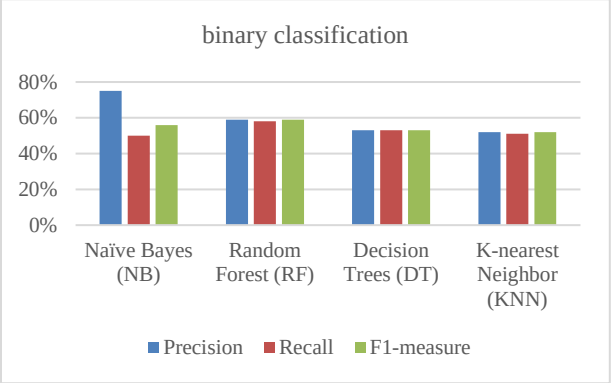

Fig. 10 shows the results of prediction (binary classification)

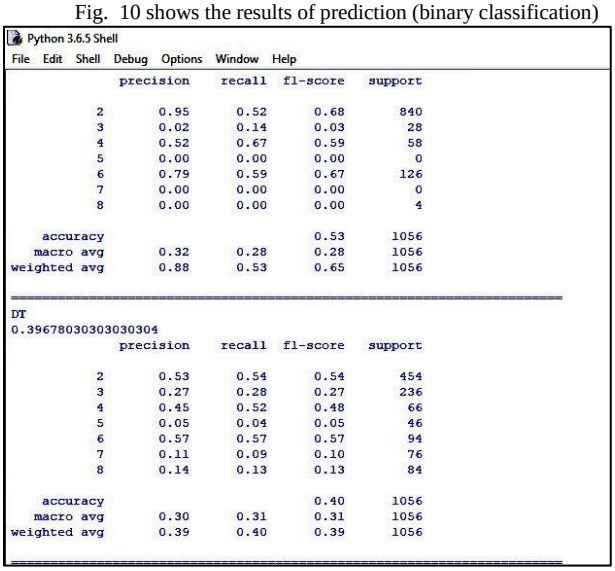

Python 3.6.5 Shell

File Edit Shell Debug Options Window Help

	precision	recall	f1-score	support
2	0.95	0.52	0.68	840
3	0.02	0.14	0.03	28
4	0.52	0.67	0.59	58
5	0.00	0.00	0.00	0
6	0.79	0.59	0.67	126
7	0.00	0.00	0.00	0
8	0.00	0.00	0.00	4
accuracy			0.53	1056
macro avg	0.32	0.28	0.28	1056
weighted avg	0.88	0.53	0.65	1056

DT
0.39678030303030304

	precision	recall	f1-score	support
2	0.53	0.54	0.54	454
3	0.27	0.28	0.27	236
4	0.45	0.52	0.48	66
5	0.05	0.04	0.05	46
6	0.57	0.57	0.57	94
7	0.11	0.09	0.10	76
8	0.14	0.13	0.13	84
accuracy			0.40	1056
macro avg	0.30	0.31	0.31	1056
weighted avg	0.39	0.40	0.39	1056

Fig 11

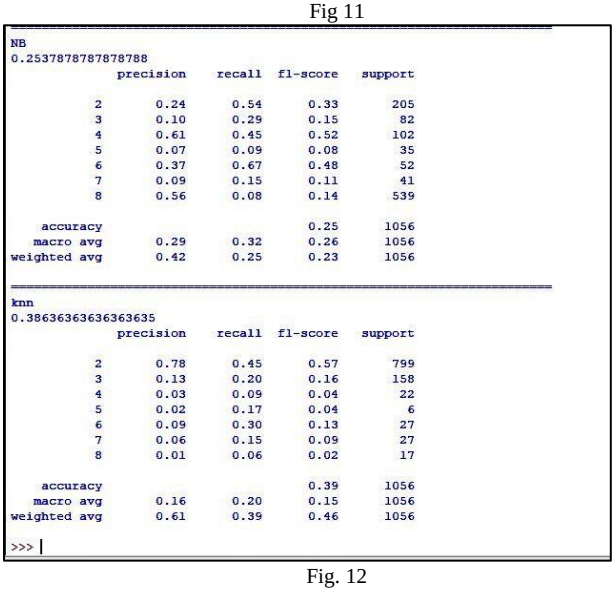

NB
0.2537878787878788

	precision	recall	f1-score	support
2	0.24	0.54	0.33	205
3	0.10	0.29	0.15	82
4	0.61	0.45	0.52	102
5	0.07	0.09	0.08	35
6	0.37	0.67	0.48	52
7	0.09	0.15	0.11	41
8	0.56	0.08	0.14	539
accuracy			0.25	1056
macro avg	0.29	0.32	0.26	1056
weighted avg	0.42	0.25	0.23	1056

knn
0.38636363636363635

	precision	recall	f1-score	support
2	0.78	0.45	0.57	799
3	0.13	0.20	0.16	158
4	0.03	0.09	0.04	22
5	0.02	0.17	0.04	6
6	0.09	0.30	0.13	27
7	0.06	0.15	0.09	27
8	0.01	0.06	0.02	17
accuracy			0.39	1056
macro avg	0.16	0.20	0.15	1056
weighted avg	0.61	0.39	0.46	1056

>>>

Fig. 12

Fig. (11,12)shows the results of multi classification

TABLE IV
CLASSIFIER'S PERFORMANCE ON THE CLASSIFICATION ALGORITHMS

classification algorithms (multi classification)	Precision	Recall	F1-measure
Random Forest (RF)	88%	53%	65%
K-nearest Neighbor (KNN)	61%	39%	46%
Naïve Bayes (NB)	42%	25%	23%
Decision Trees (DT)	39%	40%	39%

As illustrated in the previous table the results show precision values in the (ODIR) dataset that appears the RF algorithm scored the highest precision in ML(machine learning) algorithms that is 88% compared to the KNN algorithm that achieves 61%, the NB algorithm that achieves 42% and the DT algorithm that achieves 39% in case of multi classification.

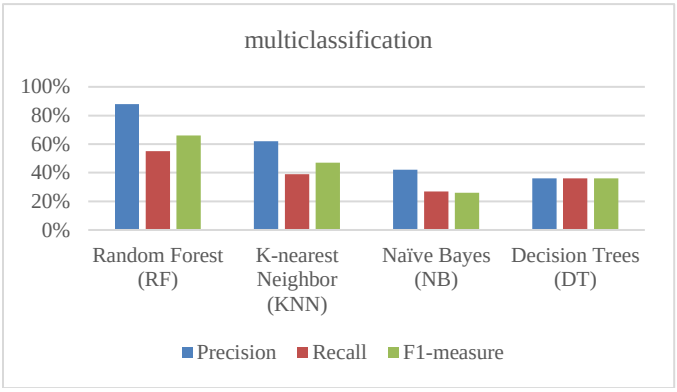

Fig. 13 shows the results of prediction (multi classification)

IX. CONCLUSION

The model in this work was utilized for classifying the major ocular disease and predict whether an eye has a disease or a healthy fundus. ODIR data-set, which contains 5,000 images of 8 different types of fundus. The many ocular illnesses have been represented by those classes, was classified by using ML methods. Additionally, the performance much exceeds expectations. This study achieved the highest accuracy for binary classification (abnormal and normal) which is 75% (NB algorithm), 62% (RF algorithm), 53% (KNN algorithm), 51% (DT algorithm) and achieved the highest accuracy for multiclass classification (types of eye diseases) which is 88% (RF algorithm), 61% (KNN algorithm) 42% (NB algorithm), and 39% (DT algorithm). Such a method will revolutionize the field of eye disease diagnosis and be of great use to medical professionals. We believe that it could still be a useful model and that there are chances for improvement with additional research and investigation in the near future.

REFERENCES

[1] Y. Elloumi, M. Akil, and H. Boudegga, "Ocular diseases diagnosis in fundus images using a deep learning: approaches, tools and performance evaluation," *Maryland, USA, p. 109960T*, p. 30, 2019,

doi: 10.1117/12.2519098.

[2] M. S. Khan *et al.*, "Deep learning for ocular disease recognition: an inner-class balance," *Comput. Intell. Neurosci.*, vol. 2022, 2022.

[3] A. O. Adio, A. Alikor, and E. Awoyesuku, "Survey of pediatric ophthalmic diagnoses in a teaching hospital in Nigeria.," *Niger. J. Med.*, vol. 20, no. 1, pp. 105–108, 2011.

[4] K. Prasad, P. S. Sajith, M. Neema, L. Madhu, and P. N. Priya, "Multiple eye disease detection using Deep Neural Network," in *IEEE Region 10 Annual International Conference, Proceedings/TENCON*, IEEE, 2019, pp. 2148–2153. doi: 10.1109/TENCON.2019.8929666.

[5] N. Gour and P. Khanna, "Multi-class multi-label ophthalmological disease detection using transfer learning based convolutional neural network," *Biomed. Signal Process. Control*, vol. 66, p. 102329, 2021, doi: 10.1016/j.bspc.2020.102329.

[6] N. Badah, A. Algefes, A. AlArjani, and R. Mokni, "Automatic eye disease detection using machine learning and deep learning models," in *Pervasive Computing and Social Networking: Proceedings of ICPCSN 2022*, Springer, 2022, pp. 773–787.

[7] K. Plataniotis and A. N. Venetsanopoulos, *Color image processing and applications*. Springer Science & Business Media, 2000.

[8] R. Bala and K. M. Braun, "Color-to-grayscale conversion to maintain discriminability," in *Color Imaging IX: Processing, Hardcopy, and Applications*, SPIE, 2003, p. 196. doi: 10.1117/12.532192.

[9] G. Iwasokun, "Image Enhancement Methods: A Review," *Br. J. Math. Comput. Sci.*, vol. 4, no. 16, pp. 2251–2277, 2014, doi: 10.9734/bjmcs/2014/10332.

[10] M. Sharma, R. B. Dubey, and S. Gupta, "Feature extraction of mammograms," *Int. J. Adv. Comput. Res.*, vol. 2, no. 3, p. 10, 2012.

[11] B. K. Elfarra and I. S. Abuhaiba, "Mammogram computer aided diagnosis," *Int. J. Signal Process. Image Process. Pattern Recognit.*, vol. 5, no. 4, pp. 1–30, 2012.

[12] A. R. Abed, "Implementation of Deep Learning Model for Breast Cancer Diagnosis," 2022.

[13] W. Zhang, W. Quan, and L. Guo, "Blurred star image processing for star sensors under dynamic conditions," *Sensors (Switzerland)*, vol. 12, no. 5, pp. 6712–6726, 2012, doi: 10.3390/s120506712.

[14] B. K. Triwijoyoa and A. Adila, "Analysis of medical image resizing using bicubic interpolation algorithm," *J. Ilmu Komput*, vol. 14, no. 2, pp. 20–29, 2021.

[15] G. M. S. Najah and G. Şengül, "Emotion estimation from facial images," *Atilim Univ.*, vol. 10, 2017.

[16] S. Seeger and X. Laboureux, "Feature extraction and registration: An overview," *Princ. 3D image Anal. Synth.*, pp. 153–166, 2002.

[17] D. G. Lowe, "Object recognition from local scale-invariant features," in *Proceedings of the IEEE International Conference on Computer Vision*, Ieee, 1999, pp. 1150–1157. doi: 10.1109/iccv.1999.790410.

[18] D. G. Lowe, "Distinctive image features from scale-invariant keypoints," *Int. J. Comput. Vis.*, vol. 60, pp. 91–110, 2004.

[19] Y. Y. Wang, Z. M. Li, L. Wang, and M. Wang, "A scale Invariant Feature Transform based method," *J. Inf. Hiding Multimed. Signal Process.*, vol. 4, no. 2, pp. 73–89, 2013.

[20] W.-J. Yang, W.-H. Du, P.-C. Chang, J.-F. Yang, and P.-H. Hung, "Visual thing recognition with binary scale-invariant feature transform and support vector machine classifiers using color information," *Int. J. Comput. Inf. Eng.*, vol. 11, no. 6, pp. 789–793, 2017.

[21] S.-I. Bejinariu and R. Luca, "Analysis of Abnormal Crowd Movements based on Features Tracking," *Rom. J. Inf. Sci. Technol.*, vol. 21, no. 2, pp. 193–205, 2018.

[22] S.-I. Bejinariu, H. Costin, F. Rotaru, R. Luca, C. D. Niţă, and C. Lazăr, "Fireworks algorithm based image registration," in *Soft Computing Applications: Proceedings of the 7th International Workshop Soft Computing Applications (SOFA 2016), Volume 1 7*, Springer, 2018, pp. 509–523.

[23] M. H. Vardhan and S. V. Rao, "GLCM architecture for image extraction," *Int. J. Adv. Res. Electron. Commun. Eng*, vol. 3, pp. 75–82, 2014.

[24] C.-C. Gao and X.-W. Hui, "GLCM-based texture feature extraction," *Comput. Syst. Appl.*, vol. 19, no. 6, pp. 195–198, 2010.

[25] R. M. Haralick, K. Shanmugam, and I. H. Dinstein, "Textural features for image classification," *IEEE Trans. Syst. Man. Cybern.*, no. 6, pp. 610–621, 1973.

[26] D. Sisodia and D. S. Sisodia, "Prediction of Diabetes using Classification Algorithms," *Procedia Comput. Sci.*, vol. 132, pp. 1578–1585, 2018, doi: 10.1016/j.procs.2018.05.122.

[27] I. Rish, "An empirical study of the naive Bayes classifier," in *IJCAI 2001 workshop on empirical methods in artificial intelligence*, 2001, pp. 41–46.

[28] S. Zhang, X. Li, M. Zong, X. Zhu, and R. Wang, "Efficient kNN classification with different numbers

of nearest neighbors," *IEEE Trans. neural networks Learn. Syst.*, vol. 29, no. 5, pp. 1774–1785, 2017.

[29] B. Charbuty and A. Abdulazeez, "Classification based on decision tree algorithm for machine learning," *J. Appl. Sci. Technol. Trends*, vol. 2, no. 01, pp. 20–28, 2021.

[30] B. Hssina, A. Merbouha, H. Ezzikouri, and M. Erritali, "A comparative study of decision tree ID3 and C4. 5," *Int. J. Adv. Comput. Sci. Appl.*, vol. 4, no. 2, pp. 13–19, 2014.

[31] N. Schnitzler, P.-S. Ross, and E. Gloaguen, "Using machine learning to estimate a key missing geochemical variable in mining exploration: Application of the Random Forest algorithm to multi-sensor core logging data," *J. Geochemical Explor.*, vol. 205, p. 106344, 2019.

[32] M. Xiao, L. A. Wu, and H. J. Kimble, "Precision measurement beyond the shot-noise limit," *Phys. Rev. Lett.*, vol. 59, no. 3, pp. 278–281, 1987, doi: 10.1103/PhysRevLett.59.278.

[33] M. Toepfer and C. Seifert, "Content-based quality estimation for automatic subject indexing of short texts under precision and recall constraints," in *Digital Libraries for Open Knowledge: 22nd International Conference on Theory and Practice of Digital Libraries, TPDL 2018, Porto, Portugal, September 10–13, 2018, Proceedings 22*, Springer, 2018, pp. 3–15.

[34] S. Ghannay, A. Caubriere, Y. Esteve, A. Laurent, and E. Morin, "End-to-end named entity extraction from speech," *arXiv Prepr. arXiv1805.12045*, 2018.